NeuroImage 68 (2013) 63–74

Contents lists available at SciVerse ScienceDirect

NeuroImage

journal homepage: www.elsevier.com/locate/ynimg

Brain development and aging: Overlapping and unique patterns of change

Christian K. Tamnes [a,*], Kristine B. Walhovd [a], Anders M. Dale [b,c,d], Ylva Østby [a], Håkon Grydeland [a], George Richardson [b], Lars T. Westlye [a], J. Cooper Roddey [b], Donald J. Hagler Jr. [b,c], Paulina Due-Tønnessen [e], Dominic Holland [b,d], Anders M. Fjell [a]
and the Alzheimer's Disease Neuroimaging Initiative [1]

[a] Center for the Study of Human Cognition, Department of Psychology, University of Oslo, Oslo, Norway
[b] Multimodal Imaging Laboratory, University of California, San Diego, CA, USA
[c] Department of Radiology, University of California, San Diego, CA, USA
[d] Department of Neurosciences, University of California, San Diego, CA, USA
[e] Department of Radiology, Rikshospitalet, Oslo University Hospital, Oslo, Norway

ARTICLE INFO

Article history:
Accepted 20 November 2012
Available online 12 December 2012

Keywords:
Adolescence
Longitudinal
Maturation
MRI
Neuroimaging
Retrogenesis

ABSTRACT

Early-life development is characterized by dramatic changes, impacting lifespan function more than changes in any other period. Developmental origins of neurocognitive late-life functions are acknowledged, but detailed longitudinal magnetic resonance imaging studies of brain maturation and direct comparisons with aging are lacking. To these aims, a novel method was used to measure longitudinal volume changes in development (n = 85, 8–22 years) and aging (n = 142, 60–91 years). Developmental reductions exceeded 1% annually in much of the cortex, more than double to that seen in aging, with a posterior-to-anterior gradient. Cortical reductions were greater than the subcortical during development, while the opposite held in aging. The pattern of lateral cortical changes was similar across development and aging, but the pronounced medial temporal reduction in aging was not precast in development. Converging patterns of change in adolescents and elderly, particularly in the medial prefrontal areas, suggest that late developed cortices are especially vulnerable to atrophy in aging. A key question in future research will be to disentangle the neurobiological underpinnings for the differences and the similarities between brain changes in development and aging.

Introduction

Despite increasing recognition of the importance of developmental processes for later neurocognitive functions (Deary et al., 2006; Kochunov et al., 2012), and neurodegenerative (Shaw et al., 2007) and neuropsychiatric (Gogtay et al., 2011; Paus et al., 2008) disorders, studies directly comparing brain changes in development and aging are lacking. Human brain development is notably protracted (Blakemore, 2012; Giedd and Rapoport, 2010; Jernigan et al., 2011), and much of the potential and many of the vulnerabilities of the brain depend on the first two decades of life (Toga et al., 2006). It is even suggested that common mechanisms may be implicated in brain maturation in childhood and degenerative changes in aging (Nikolaev et al., 2009; Wines-Samuelson and Shen, 2005), reflected in potentially more age-related atrophy in regions characterized by higher degree of plasticity during development (Mesulam, 2000; Toga et al., 2006). Still, testing of similarities and differences between patterns of change in development and healthy aging has not been undertaken. Thus, the purpose of the present study was to characterize developmental trajectories across childhood and adolescence in both the cerebral cortex and a range of subcortical structures, test how the pattern of maturation changes across development, and directly compare this to the pattern of atrophy in a sample of elderly.

Developmental magnetic resonance imaging (MRI) studies show that while the first years of life are characterized by gray matter (GM) increases (Gilmore et al., 2012; Knickmeyer et al., 2008), older children and adolescents show cortical GM decreases in most regions, increasing white matter (WM) volumes and heterogeneous changes in subcortical structures (Brain Development Cooperative Group, 2012; Brown et al., 2012; Giedd et al., 1996a, 1999; Lenroot et al., 2007; Muftuler et al., 2011; Østby et al., 2009; Sowell et al., 2004; Tamnes et al., 2010; Westlye et al., 2010b). Longitudinal studies with wide age-ranges are needed, however, as they allow modulation of differences in change-patterns across age, for instance enabling testing of the posterior–anterior theory of cortical maturation, which suggests that

* Corresponding author at: Department of Psychology, University of Oslo, PO Box 0194 Blindern, 0317 Oslo, Norway. Fax: +47 22845001.
E-mail address: c.k.tamnes@psykologi.uio.no (C.K. Tamnes).

[1] Some of the data used in the preparation of this article were obtained from the Alzheimer's Disease Neuroimaging Initiative (ADNI) database (adni.loni.ucla.edu). As such, the investigators within the ADNI contributed to the design and implementation of ADNI and/or provided data, but did not participate in the analysis or writing of this report. A complete listing of ADNI investigators can be found at: adni.loni.ucla.edu.

1053-8119/$ – see front matter © 2012 Elsevier Inc. All rights reserved.
http://dx.doi.org/10.1016/j.neuroimage.2012.11.039

higher-order association cortices mature relatively late (Gogtay et al., 2004; Shaw et al., 2008). Moreover, simultaneous measurements of cortical and subcortical structures yield a unique possibility for characterizing the pattern of variation in developmental trajectories across anatomical areas (Østby et al., 2009). In a benchmark study, Shaw et al. (2008) found differing levels of complexity of developmental trajectories across the cortex and that this pattern aligned with the cortical types depicted in established cytoarchitectonic maps. Subcortical changes were not investigated, however. Furthermore, studies combining samples of children and elderly are necessary to test how developmental trajectories align with the pattern of atrophy in aging. Similar to development, a heterogeneous pattern of atrophy is seen in healthy aging, with the frontal and temporal regions showing the largest changes (Fjell and Walhovd, 2010; Lemaitre et al., 2012).

Here, we present analyses of longitudinal MRI data obtained from 85 children and adolescents (8–22 years), and compare developmental cortical and subcortical changes with atrophy in 142 healthy elderly participants (60–91 years) (Fjell et al., 2009a). The aims of the current study were to 1) characterize developmental changes in cortical and subcortical structures, 2) test how the pattern of maturation changes across development, and 3) directly contrast changes in development and aging. An accurate description of healthy brain development and detailed knowledge of individual differences in developmental trajectories are paramount to understanding the foundations of cognitive development, neurodevelopmental disorders, and later lifespan changes. We used a novel unbiased method to quantify volumetric change (Holland and Dale, 2011) that has been proven to be highly sensitive to even subtle changes over short time periods in elderly participants (Holland et al., 2012; Murphy et al., 2010), but which has never before been used in developing samples. Furthermore, this was combined with image segmentation and parcellation to obtain change estimates in a large number of cortical and subcortical regions.

Material and methods

Participants

The sample of children and adolescents was drawn from the longitudinal project *Neurocognitive Development* (Østby et al., 2009; Tamnes et al., 2010), University of Oslo. The study was approved by the Regional Ethical Committee of South Norway. Typically developing children and adolescents aged 8–19 years were recruited through newspaper ads and local schools. Written informed consent was obtained from all participants older than 12 years of age and from a parent for participants under 16 years of age. Oral informed consent was given by participants under 12 years of age. Parents and participants aged 16 years or older were at both time-points screened with separate standardized health interviews to ascertain eligibility. Participants were required to be right handed, fluent Norwegian speakers, have normal or corrected to normal vision and hearing, not have a history of injury or disease known to affect central nervous system (CNS) function, including neurological or psychiatric illness or serious head trauma, not be under psychiatric treatment, not use psychoactive drugs known to affect CNS functioning, not have had complicated or premature birth, and not have MRI contraindications. Additionally, all scans were evaluated by a neuroradiologist at both time-points and required to be deemed free of significant injuries or conditions.

At time-point 1 (tp1), 111 participants satisfied these criteria and had adequate processed and quality checked MRI data. Eighteen participants did not want to or were unable to participate at time-point 2 (tp2), two were not located, three had dental braces and three were excluded due to neurological or psychiatric conditions. Thus, at tp2, 85 participants (38 females) underwent a second MRI scan. The mean age at tp1 for this final sample was 13.7 years (SD = 3.4, range = 8.2–19.4) and the mean IQ, as assessed by the Wechsler Abbreviated Scale of Intelligence (WASI) (Wechsler, 1999), was 109.0 (SD = 11.4, range = 82–141). The mean age at tp2 was 16.3 years (SD = 3.4, range = 10.8–21.9) and the mean IQ was 112.5 (SD = 10.5, range = 87–136). The mean interval between the two scanning sessions was 2.6 years (SD = 0.2, range = 2.4–3.2). The length of the interval was not related to age ($r = -.03$, $p = .772$) and not different for girls and boys ($t = 0.42$, $p = .675$).

The sample of healthy elderly was originally obtained from the Alzheimer's Disease Neuroimaging Initiative (ADNI) database (adni.loni.ucla.edu), and has previously been reported by Fjell et al. (2009a), but has not previously been used as in the current study. The total number of participants entering ADNI as healthy controls at baseline, and who attended the one year follow-up was 204. ADNI eligibility criteria are described at www.adni-info.org. Briefly, participants were 55–91 years of age, had an informant able to provide an independent evaluation of functioning, spoke either English or Spanish and had Mini-Mental State Examination (MMSE) (Folstein et al., 1975) scores between 24 and 30 (inclusive) and a Clinical Dementia Rating (CDR) (Morris, 1993) of 0. Of these 204, only those with MR segmentation passing internal quality control for baseline, one year follow-up and processing of change were included, and we additionally excluded those that had worse CDR sum of boxes score at the time of follow-up. The final sample consisted of 142 participants (tp1 mean age = 75.6 years, range = 59.8–90.2 years, 68 females), which were followed for one year (tp2 mean age = 76.7 years, range = 60.8–91.3 years).

MRI acquisition

Imaging data on children and adolescents were collected using a 12 channel head coil on a 1.5 T Siemens Avanto scanner (Siemens Medical Solutions) at Rikshospitalet, Oslo University Hospital. The same scanner and sequences were used at both time-points. The pulse sequences used for morphometry analysis were two repeated 160 slice sagittal T1-weighted magnetization prepared rapid gradient echo (MPRAGE) sequences (time repetition (TR)/time echo (TE)/time to inversion (TI)/flip angle (FA) = 2400 ms/3.61 ms/1000 ms/8°) per participant per visit. To increase the signal-to-noise ratio (SNR) the two runs were averaged during pre-processing. The protocol also included a 176 slice sagittal 3D T2-weighted turbo spin-echo sequence (TR/TE = 3390/388 ms) and a 25 slice coronal FLAIR sequence (TR/TE = 7000–9000/109 ms) to aid the neuroradiological examination.

All ADNI scans used for comparison purposes in the present paper were from 1.5 T scanners. Data were collected across a variety of scanners with protocols and acquisition parameters standardized across platforms, as described in detail at adni.loni.ucla.edu/research/protocols/mri-protocols/mri-protocols-adni-1. A major effort has been devoted to evaluating and adjusting the sequences for morphometric analyses (Jack et al., 2008). For the sample included in the current study, raw DICOM MRI scans (including two T1-weighted volumes per case) were downloaded from the ADNI site. Consequently, while all the MRI data from the children and adolescents were acquired on the same scanner using the same sequence, different scanners were used across subjects in the healthy elderly sample. Although this constitutes a caveat and potential source of bias, previous studies have shown that brain morphometry can be reliably estimated across a number of image acquisition variables (Han et al., 2006; Jovicich et al., 2009), as well as consistent age-related differences in elderly participants across multiple samples (Fjell et al., 2009b; Walhovd et al., 2011).

MRI analysis

Image processing and analyses were performed at the Multimodal Imaging Laboratory, University of California, San Diego. The raw data were reviewed for quality, and automatically corrected for spatial distortion due to gradient nonlinearity (Jovicich et al., 2006) and B_1

field inhomogeneity (Sled et al., 1998). The two image volumes for each participant were co-registered, averaged to improve the SNR, and resampled to isotropic 1-mm voxels. Volumetric segmentation (Fischl et al., 2002) and cortical surface reconstruction (Dale et al., 1999; Fischl and Dale, 2000; Fischl et al., 1999) and parcellation (Desikan et al., 2006; Fischl et al., 2004), using the FreeSurfer software package (version 5.1.0; Martinos Center for Biomedical Imaging, Boston, MA), were used to quantify the volumes of brain regions, as described in detail elsewhere (Fennema-Notestine et al., 2009; Holland et al., 2009). The subcortical segmentation and surface reconstruction and parcellation procedures are run automatically, but require supervision of the accuracy of spatial registration and tissue segmentations. All volumes were inspected for accuracy and minor manual edits were performed by a trained operator on the baseline images for nearly all subjects, usually restricted to the removal of nonbrain tissue included within the cortical boundary.

Longitudinal changes in brain structure measures were quantified by QUARC (Quantitative Anatomical Regional Change) (Holland and Dale, 2011; Holland et al., 2009; McEvoy et al., 2011; Thompson and Holland, 2011), developed at the Multimodal Imaging Laboratory, University of California, San Diego. For each participant, dual 3-D follow-up structural scans were rigid-body aligned, averaged and affine aligned to the participant's baseline. A deformation field was calculated from a nonlinear registration (Holland and Dale, 2011). The images are heavily blurred (smoothed), making them almost identical, and a merit or potential function was calculated. This merit function expresses the intensity difference between the images at each voxel, and depends on the displacement field for the voxel centers of the image being transformed; it is also regularized to keep the displacement field spatially smooth. The merit function by design will have a minimum when the displacement field induces a good match between the images. It is minimized efficiently using standard numerical methods. Having found a displacement field for the heavily blurred pair of images, the blurring is reduced and the procedure is repeated, thus iteratively building up a better displacement field. Two important additions to this are: 1) applying the final displacement field to the image being transformed, then nonlinearly registering the resultant image to the same target, and finally tracing back through the displacement field thus calculated to find the net displacement field; and 2) restricting the displacement fields to regions of interest and zooming when structures are separated by only a voxel or two. These additional features enable very precise registration involving large or subtle deformations, even at small spatial scales with low boundary contrast. Although large deformations are allowed by multiple nonlinear registration (or relaxation) steps, nonphysical deformations are precluded because at each level of blurring the image undergoing deformation is restricted to conform to the target. Note that calculating the deformation field does not depend on initially segmenting tissue. This deformation field was used to align scans at the sub-voxel level. Furthermore, this was combined with image segmentation and parcellation to obtain volume change estimates in a large number of cortical and subcortical regions.

The second time-point was used as baseline, as it is reasonable to assume that there is less motion distortion with older age in developmental samples. To ease the interpretation of the results, the direction of all effects was inversed in the surface illustrations. Subcortical segmentation and cortical parcellation labels from the tp2 images were used to extract the average volume change for each ROI. For all ROIs, the annual percentage volume change from tp1 was calculated prior to statistical analyses. The FreeSurfer segmentation and parcellation techniques were used as they allowed us to map longitudinal changes in a large number of subcortical structures and anatomically meaningful cortical regions. The scans from the healthy elderly participants were processed very similarly to the current protocol, as described in detail elsewhere (Fjell et al., 2009a). QUARC has previously been applied to serial pairs of scans from elderly participants and proven to be highly sensitive to even subtle changes over short time periods (Fjell et al., 2009a; Holland et al., 2012; Murphy et al., 2010).

Statistical analyses

Statistical analyses were performed by use of FreeSurfer 5.1 (http://surfer.nmr.mgh.harvard.edu/) and PASW Statistics 18.0, and curve fitting was performed using functions freely available through the statistical environment R (http://www.r-project.org/). Longitudinal change in cortical and subcortical brain volumes was calculated as the percentage change relative to baseline. Cortical analyses across the surface were performed with general linear models (GLMs) as implemented in FreeSurfer and results were displayed on a semi-inflated template brain. In the developmental sample ($n = 85$, 8–22 years), we first tested whether cortical changes were significantly different from zero. Second, the statistical significance of the effects of sex on cortical volume change was tested. Third, we tested the effects of age on change to investigate if the rate of cortical change differed across the studied age-span. To visualize how cortical change differed across age, the annualized rate of change (%) and standardized rate of change (Z-score) across each hemisphere were estimated per year and smoothed across the age-range by use of a smoothing spline approach (Fjell et al., 2010a). Finally, the significance of the effects of the interaction term age × sex on cortical volume change was tested, with age and sex included as covariates. Scan interval was included as a covariate in all GLMs. The surface significance maps were thresholded by a conventional criterion for correction for multiple comparisons (false discovery rate (FDR) at the 5% level) (Genovese et al., 2002).

For the ROI-data from the developmental sample, initial paired samples t-tests were performed to compare longitudinal change in the left and right hemispheres. To reduce the number of ROIs in further analyses, mean change values of the left and right hemisphere ROIs were used. One-sample t-tests were used to test whether longitudinal change within each of the 47 ROIs was different from zero and independent samples t-tests were used to compare change in girls and boys. Next, Pearson correlations were performed between age and change in each ROI. All ROI results were Bonferroni-corrected by a factor of 47 (reflecting the number of ROIs), roughly corresponding to a corrected alpha of $p < 0.001$. To illustrate volumetric change within individuals, spaghetti plots of volume by age were created for each ROI. As global fits such as quadratic models may be affected by irrelevant factors, such as the sampled age-range (Fjell et al., 2010a), an assumption-free longitudinal nonparametric general additive model for each ROI as a function of age was fitted to accurately describe changes across the studied age-range.

Longitudinal change and the effects of age on change are not reported for the healthy elderly sample separately, as this has been published previously (Fjell et al., 2009a). However, to characterize brain structure changes in development in a life-span perspective, regional annual percentage volume changes were compared between the current sample ($n = 85$, 8–22 years) and the sample of healthy elderly participants ($n = 142$, 60–91 years). To visualize the cortical areas that showed more and less than average longitudinal change in development and aging, respectively, the surface maps were z-transformed for each hemisphere in each sample separately by subtracting the mean rate of change and dividing by the standard deviation of change. Finally, we calculated the differences between the smoothed estimated Z-score maps in early development (age 8) vs. aging (age 75) and late development (age 20) vs. aging (age 75). Note that the estimated Z-score maps at these selected ages were smoothed across the age-range (Fjell et al., 2010a), and thus not dependent on the subjects only at these specific ages, but rather represent a sort of weighted average of the ages around the selected points.

Results

Longitudinal developmental change: continuous surface analyses

When a commonly used approach to correct for multiple comparisons was employed (FDR 5%, corresponding to $p<.045$), significant volume changes were observed across almost the entire cortical surface in development ($n=85$, 8–22 years). Thus, a more conservative threshold ($p<10^{-5}$) was used to allow differentiation of effects. Highly significant volume reductions were still evident across almost all cortical regions (Fig. 1). Annual percentage volume reductions varied across the cortex, but exceeded 1.0% in many locations (Fig. 1). Changes were most prominent bilaterally in the dorsolateral prefrontal, posterior part of the lateral temporal, inferior parietal, supramarginal and precuneus cortices, where annual reductions generally exceeded 1.5%. There were no significant effects of sex on cortical volume change. We also visually compared the annual percentage volume change across the surface in girls and boys, and the effects were very similar.

Longitudinal developmental change: ROI analyses

For the regions of interest (ROI) data, we first tested for hemisphere differences in annual percentage change by means of paired samples t-tests. None of the subcortical or ventricular ROIs showed significant hemisphere differences in change rates. For the 33 cortical surface ROIs, five temporal and medial parietal regions showed significantly ($p<.001$) larger percent volume declines in the left hemisphere: superior temporal (−1.02 vs −0.89), inferior temporal (−1.18 vs −1.04), transverse temporal (−0.86 vs −0.72), paracentral (−0.85 vs −0.71) and precuneus (−1.40 vs −1.32), and four frontal and lateral parietal regions showed larger decreases in the right hemisphere: rostral middle frontal (−1.32 vs −1.19), pars triangularis (−1.26 vs −1.10), inferior parietal (−1.64 vs −1.51) and supramarginal (−1.55 vs −1.40). Although statistically significantly different, the change rates in these ROIs were rather similar across the two hemispheres. Thus, to reduce the number of comparisons, the mean values from the two hemispheres were used in the further main ROI-analyses, and the readers are referred to the continuous surface analyses and Supplementary Table 1 for inspections of hemispheric effects.

The annual percentage volume change in each of the 47 ROIs was calculated (Table 1) and spaghetti plots of volume by age for the total cerebral cortex, the subcortical structures and selected cortical regions were created (Fig. 2). The total cerebral cortex showed remarkably consistent change across individuals, with volume reduction seen in nearly all participants. Of the subcortical structures, the caudate (−0.82) showed the largest annual percentage reduction, followed by the accumbens (−0.62), the putamen (−0.60), the cerebellum cortex (−0.58) and the thalamus (−0.44). Smaller decreases were observed in the pallidum (−0.20), hippocampus (−0.16) and amygdala (−0.16, not significant), while the brainstem (0.52) increased in volume. The lateral ventricles (1.92) showed large increases, while no significant changes were found in the inferior lateral, third or fourth ventricles. All surface ROIs showed significant volume reductions, except the entorhinal cortex and temporal pole, where no significant changes were found. Of the cortical regions, the inferior parietal (−1.57), supramarginal (−1.47), banks of the superior temporal sulcus (−1.43), precuneus (−1.36), middle temporal (−1.30), and rostral middle frontal (−1.26) changed the most. Independent samples t-tests showed no significant sex differences in annual percentage change in any of the ROIs.

Temporal patterns in developmental change rates

To investigate if the rate of cortical change differed across the studied age-span in the sample of children and adolescents ($n=85$, 8–22 years), we performed GLMs testing the statistical significance of the effects of age on volume change across the surface. The results (Fig. 3) showed significantly more change as a function of age bilaterally in the precentral, superior frontal, frontal pole and anterior temporal areas, and significantly more change at younger age bilaterally in selected parietal, occipital and posterior insular areas. Almost the entire cortical surface showed volume decrease with age (see Fig. 1), but these results indicate accelerating volume reductions with higher age in selected anterior regions and decelerating reductions in several posterior regions. There were no significant effects of age × sex interactions on cortical volume change. Upon visual inspection, the effects of age on change were very similar for girls and boys.

Next, we performed correlation analyses between age and annual percentage volume change in each of the ROIs (Table 1). A negative correlation between age and change was found for one subcortical structure: the brainstem, while four cortical regions showed positive correlations: retrosplenial, precuneus, cuneus and lingual cortices, and one cortical region showed a negative correlation: the temporal pole. Additionally, the superior frontal, precentral and postcentral cortices showed uncorrected significant negative relationships between age and change ($r=-0.28$, $p\leq.01$). Note that the direction of the correlation between change and age was negative in all frontal regions and positive in all parietal and occipital regions, with the exception of the

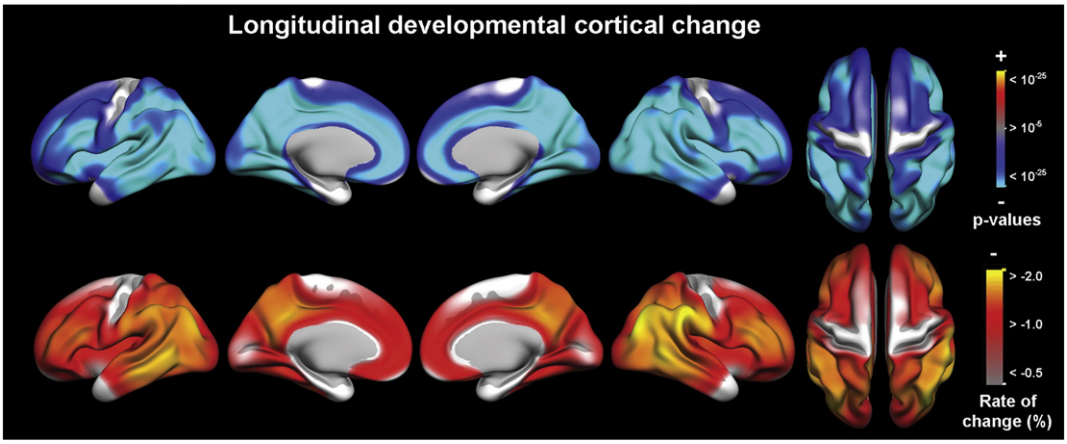

Fig. 1. Longitudinal cortical change in development. General linear models were used to test the statistical significance of cortical volume change across the brain surface in children and adolescents ($n=85$, 8–22 years), with time between the two scans included as a covariate. The significance of the effects and the rates of change were color coded and projected onto a semi-inflated template brain. The upper row shows the significance of the effects when a conservative threshold ($p<10^{-5}$) was used. The lower row shows annual percentage volume reductions.

Table 1
Annual longitudinal change and correlations between change and age in children and adolescents (n = 85, 8–22 years).

	Mean annual change			Correlation change and age	
	%	t	p	r	p
Brain structures					
Cerebral cortex	−1.15	**−20.72**	$<10^{-35}$	−0.05	.680
Cerebellum cortex	−0.58	**−11.86**	$<10^{-19}$	−0.17	.115
Accumbens	−0.62	**−11.98**	$<10^{-20}$	0.11	.317
Amygdala	−0.16	−2.85	.006	−0.25	.019
Brainstem	0.52	**8.54**	$<10^{-13}$	**−0.80**	$<10^{-20}$
Caudate	−0.82	**−16.49**	$<10^{-28}$	0.14	.206
Hippocampus	−0.16	**−4.34**	$<10^{-5}$	−0.21	.049
Pallidum	−0.20	**−5.22**	$<10^{-6}$	−0.25	.020
Putamen	−0.60	**−15.27**	$<10^{-26}$	0.06	.579
Thalamus	−0.44	**−9.44**	$<10^{-15}$	−0.33	.002
Ventricles					
Lateral ventricle	1.92	**4.49**	$<10^{-5}$	0.22	.047
Inferior lateral ventricle	0.47	1.65	.103	0.02	.835
3rd ventricle	1.03	2.42	.018	0.29	.007
4th ventricle	0.02	0.83	.934	−0.04	.697
Cortical regions					
Cingulate, rostral anterior	−0.73	**−15.18**	$<10^{-26}$	−0.11	.332
Cingulate, caudal anterior	−0.80	**−18.12**	$<10^{-31}$	−0.04	.739
Cingulate, posterior	−1.11	**−20.90**	$<10^{-35}$	0.24	.027
Cingulate, retrosplenial	−1.00	**−19.30**	$<10^{-32}$	**0.37**	$<10^{-4}$
Frontal, superior	−0.76	**−11.56**	$<10^{-19}$	−0.28	.010
Frontal, caudal middle	−0.94	**−12.58**	$<10^{-21}$	−0.23	.037
Frontal, rostral middle	−1.26	**−14.81**	$<10^{-25}$	−0.15	.172
Frontal, pars opercularis	−1.11	**−17.88**	$<10^{-30}$	−0.06	.573
Frontal, pars triangularis	−1.18	**−15.39**	$<10^{-26}$	−0.03	.764
Frontal, pars orbitalis	−0.91	**−11.99**	$<10^{-20}$	−0.08	.447
Frontal, lateral orbital	−0.84	**−15.63**	$<10^{-26}$	−0.09	.406
Frontal, medial orbital	−0.85	**−16.54**	$<10^{-28}$	−0.18	.102
Frontal, pole	−0.47	**−3.79**	$<10^{-4}$	−0.34	.001
Frontal, precentral	−0.49	**−7.24**	$<10^{-10}$	−0.28	.009
Parietal, postcentral	−0.93	**−15.82**	$<10^{-27}$	−0.28	.010
Parietal, paracentral	−0.78	**−13.04**	$<10^{-22}$	0.02	.894
Parietal, superior	−1.24	**−18.31**	$<10^{-31}$	0.28	.009
Parietal, inferior	−1.57	**−20.40**	$<10^{-34}$	0.19	.087
Parietal, supramarginal	−1.47	**−19.57**	$<10^{-33}$	0.17	.125
Parietal, precuneus	−1.36	**−22.62**	$<10^{-37}$	**0.52**	$<10^{-7}$
Temporal, parahippocampal	−0.68	**−11.39**	$<10^{-18}$	0.02	.857
Temporal, entorhinal	−0.04	−0.53	.598	−0.15	.163
Temporal, pole	0.11	1.19	.239	**−0.38**	$<10^{-4}$
Temporal, superior	−0.95	**−18.26**	$<10^{-31}$	0.06	.613
Temporal, middle	−1.30	**−16.68**	$<10^{-28}$	−0.14	.206
Temporal, inferior	−1.11	**−16.12**	$<10^{-27}$	−0.13	.240
Temporal, transverse	−0.79	**−17.85**	$<10^{-30}$	0.22	.043
Temporal, banks sup temp sulcus	−1.43	**−21.33**	$<10^{-35}$	0.22	.048
Temporal, fusiform	−0.94	**−18.10**	$<10^{-31}$	0.13	.242
Occipital, lateral	−1.10	**−16.79**	$<10^{-28}$	0.30	.006
Occipital, cuneus	−0.80	**−17.57**	$<10^{-30}$	**0.39**	$<10^{-4}$
Occipital, pericalcarine	−0.56	**−14.42**	$<10^{-24}$	0.14	.197
Occipital, lingual	−0.80	**−19.44**	$<10^{-33}$	**0.45**	$<10^{-5}$

The significance of the annual percentage volume change in each region was tested with one-sample t-tests. Pearson correlations were performed to test the associations between annual change and age. Bold: $p<.05$ (Bonferroni-corrected, factor of 47).

postcentral gyrus. This indicates a pattern of more pronounced cortical reduction at young age in the posterior areas and more pronounced reduction in adolescence in the frontal areas. The spaghetti plots of volume by age for selected cortical ROIs (Fig. 2) confirm these results, by showing slightly steeper trajectories in adolescence in the superior frontal and precentral cortices and steeper reductions in late childhood in the precuneus, retrosplenial and lingual cortices.

To delineate the effects of age on cortical change in childhood and adolescence in more detail, annualized percentage volume reduction was estimated per year and smoothed across age (Fig. 4, Video 1). A clear posterior–anterior age-gradient was seen both laterally and medially. To further illustrate the temporal pattern in cortical change, the smoothed annual percentage volume changes (shown in Fig. 4) were z-transformed across the surface for each hemisphere. The results (Fig. 5, Video 2) illustrate the areas of the cortex that show relatively higher and relatively lower rates of change at different ages. The most prominent features were a gradual relative reduction in the rate of change with increasing age in the medial parietal cortex (precuneus, retrosplenial cortex), and a gradual relative increase in the rate of change in the medial temporal and inferior parietal cortices, as well as in both the medial and lateral prefrontal cortices.

Longitudinal change in development and aging compared

Longitudinal changes and temporal patterns in change rates in the aging sample are reported elsewhere (Fjell et al., 2009a), while we here created spaghetti plots of volume by age for the total cerebral cortex and the subcortical structures (Fig. 6). Next, we compared the regional annual percentage volume change in the current sample of children and adolescents (n = 85, 8–22 years) and in the healthy elderly sample (n = 142, 60–91 years) (Table 2). While cortical reductions exceeded the subcortical in development, the tendency in aging was the opposite. Children and adolescents showed significantly larger volume reductions in the cerebral cortex and caudate, but smaller reductions in the amygdala and hippocampus. The rank order correlation between the rate of change in development and aging for the subcortical structures was −.33 (Spearman's rho), and indicates no coordination of change. Much larger ventricular volume increases were seen in aging than in development. Notably, the developmental sample showed substantially greater annual volume decreases than the aging sample in nearly all the cortical ROIs. Reductions that were at least twice as large were found in 29 of the 33 surface ROIs and reductions at least three times as large were found in 15 of the surface ROIs, including all the parietal and occipital regions. Interestingly, the only cortical regions that changed significantly more in aging compared to development were the entorhinal cortex and the temporal pole.

For the nine cortical regions that showed hemispheric differences in change rates in development (see above), we also compared the annual percentage volume change in development and aging separately for the two hemispheres (Supplementary Table 1). In all of these regions, substantially greater volume decreases were seen in development. Next, we performed analyses of variance on the annual percentage volume change in these regions to directly test if hemispheric differences in change rates were different in development and aging (Supplementary Table 1). Two of the regions showed significant hemisphere × group effects, with larger left hemisphere volume reductions in development and larger right hemisphere reductions in aging: paracentral ($F = 13.38$, $p<.001$) and inferior temporal ($F = 10.44$, $p = .001$) cortices.

To further compare the patterns of cortical volume reductions between development and aging, the annual percentage volume change was z-transformed for each hemisphere in each sample separately. The results illustrate the areas of the cortex that show relatively higher and lower rates of change within each group (Fig. 7A). Across development, higher than average volume reductions were observed in the dorsolateral prefrontal, medial parietal around the precuneus and retrosplenial cortex, lateral inferior parietal extending down to the temporo-parietal junction as well as the lateral posterior temporal and lateral occipital cortices. Within the older group, higher than average atrophy rates were most pronounced across the temporal lobes, as well as in the frontal poles and in the medial and lateral orbitofrontal cortices. Laterally, the reductions seen in development and in aging were anatomically very similar, with the exception of the anterior part of the temporal lobe, where larger than average reductions were seen in aging and smaller than average reductions were seen in development. Medially, however, there were striking differences in the pattern of change. In development, reductions in

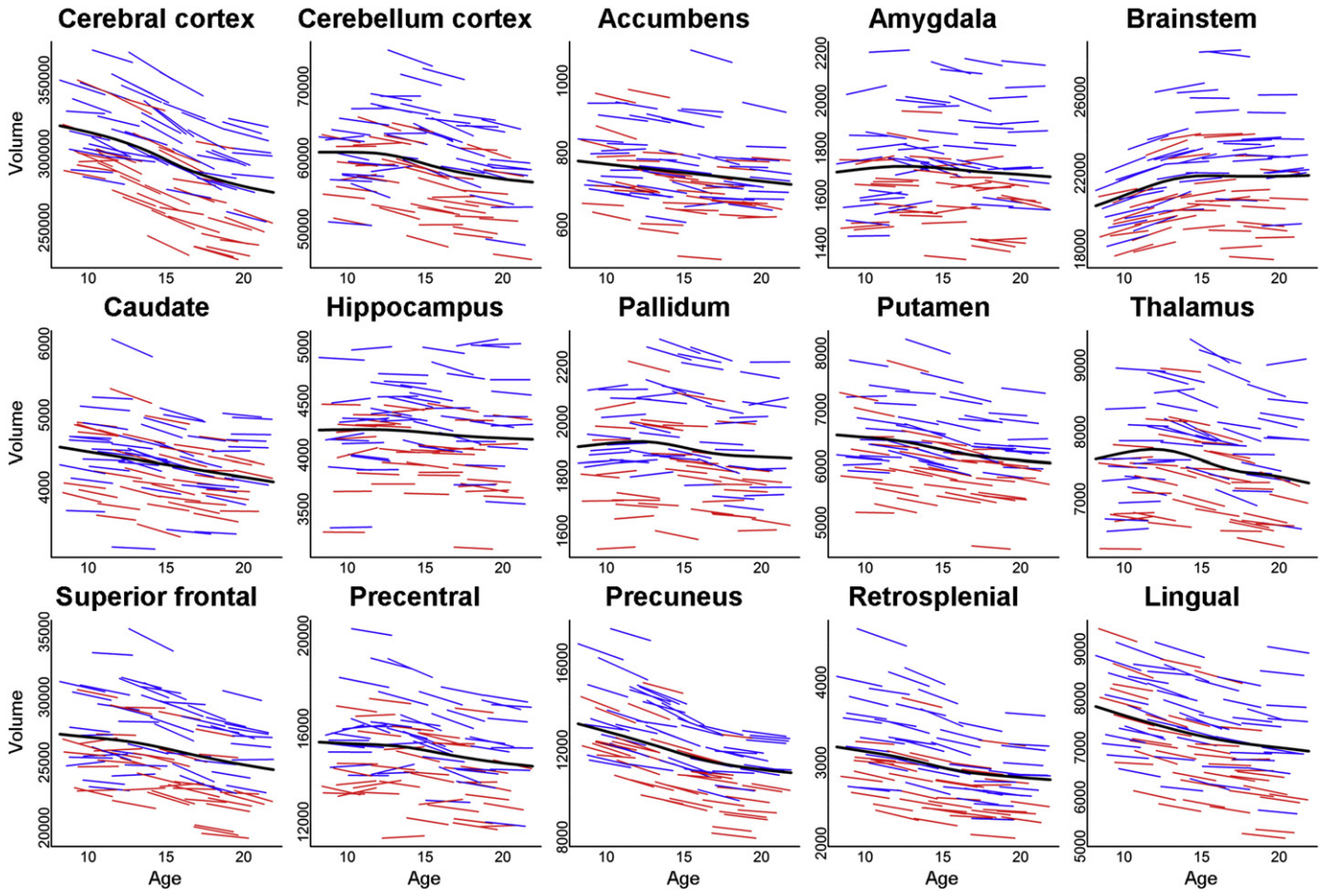

Fig. 2. Spaghetti plots for selected brain regions in development. Plots of volumes (mm^3) by age (years) for selected brain regions in the sample of children and adolescents (n = 85, 8–22 years). Volumes from the left and right hemispheres were averaged. Blue lines denote boys and red lines denote girls. For each region, an assumption-free general additive model as a function of age was fitted to accurately describe changes across the studied age-range. For the cortical regions shown in the lower row, these models indicate steeper reductions in adolescence in frontal regions (superior frontal and precentral) and steeper reductions at younger age in posterior regions (precuneus, retrosplenial and lingual).

the medial frontal lobe were of average strength and the medial temporal cortex, including the entorhinal and parahippocampal cortices, showed much less than average reductions (<2 SD). In aging, the medial orbitofrontal cortex and parts of the medial superior frontal gyrus showed up to 2 SD stronger reductions than the average cortical rate, and the same was seen for parts of the entorhinal cortex and inferior parts of the temporal cortex. Thus, the medial fronto-temporal pattern of cortical reduction characterizing healthy aging is not pronounced across development during this age-range.

To understand these differences between development and aging, it is necessary to look at the developmental trajectories. The medial fronto-temporal areas of atrophy in aging overlapped substantially with areas showing negative correlations between change and age in development (Fig. 3), i.e. areas that mature late. To directly compare early development vs. aging and late development vs. aging, we calculated the differences between the smoothed estimated Z-score maps at age 8 and at age 75, and the difference between the smoothed Z-score maps at age 20 and age 75 (Figs. 7B–C). The patterns of relative cortical changes in children and elderly participants were highly different in the medial parietal and prefrontal areas, while the relative changes in late adolescent development and aging were much more similar. However, for the medial temporal cortex, large differences in the patterns of change were seen between the group of elderly and both developmental groups.

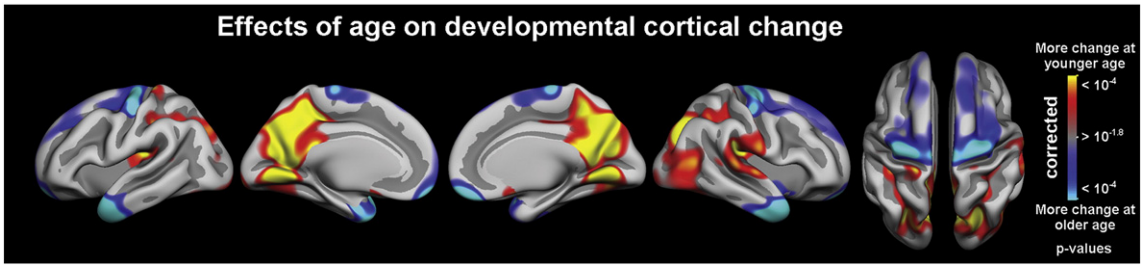

Fig. 3. Effects of age on cortical change rates in development. General linear models were used to test the significance of the effects of age on cortical volume change, with time between the two scans included as a covariate. Corrected for multiple comparisons (FDR 5%, corresponding to p<.016), blue–cyan areas indicate accelerating volume reductions with higher age, especially prominent in anterior regions, and red–yellow areas indicate decelerating reductions, especially in posterior regions.

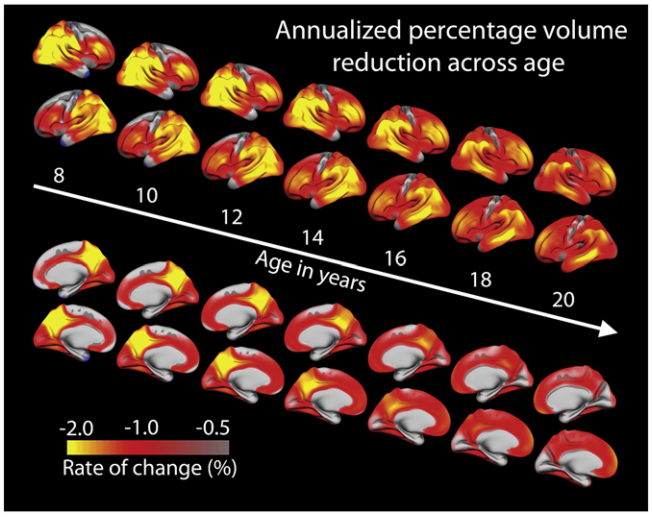

Fig. 4. Annual percentage cortical change across age in children and adolescents. Annualized percentage volume change was estimated per year and smoothed across the age-range by use of a smoothing spline approach (Fjell et al., 2010a), and shown in lateral and medial views (see also Video 1). At age 8 years, the most pronounced reductions are seen in the parietal lobes and the lateral occipital cortices. At age 20, substantial reductions are seen across most of the surface, including the frontal lobes and the anterior part of the lateral temporal lobes, but not in the medial temporal and occipital cortices. A general posterior–anterior age-gradient is seen both laterally and medially.

Discussion

The current study characterized developmental changes in cortical and subcortical volumes, tested how the pattern of maturation changes across development, and compared changes in development and aging. First, the rate of change in development was generally higher in the cerebral cortex than in the subcortical structures. Annual volume reductions exceeded 1.0% in many cortical regions, compared to changes of about 0.5% in the subcortical structures. Second, the results showed decelerating developmental change with higher age in posterior cortical areas and accelerating change in frontal areas, in line with the posterior–anterior theory of cortical maturation. For instance, change exceeding the average rate was first seen in the medial orbitofrontal cortex towards the end of the teen years. Third, a mixture of overlapping and spatially distinct patterns of change in maturation and senescence was seen. While cortical changes exceeded the subcortical in development, the tendency in aging was the opposite. Further, while the patterns of change were similar on the lateral cortical surface, the medial temporal reduction characterizing aging was not precast in development. Converging patterns of change in adolescents and elderly, particularly in the medial prefrontal cortex, support the hypothesis that late developed cortical systems are especially prone to atrophy in aging. However, the increased rate of reduction in the medial temporal cortex in aging is not mimicking developmental events. This indicates that different processes are responsible for atrophy in aging and maturational changes in these areas. The implications of the findings are discussed below.

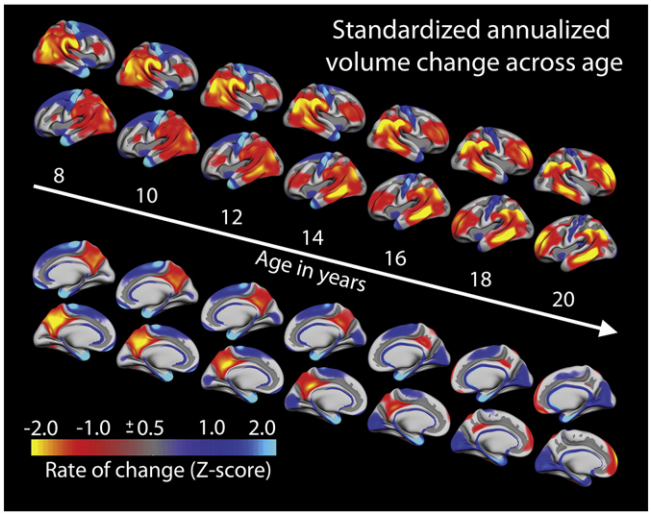

Fig. 5. Standardized cortical change across age in children and adolescents. To illustrate relatively higher and relatively lower rates of change at different ages, the smoothed annual percentage volume changes (Fig. 4) were z-transformed across the surface for each hemisphere. Red–yellow areas indicate the largest relative cortical reductions at different ages, while blue–cyan areas indicate smaller relative reductions (see also Video 2). At age 8 years, larger than average volume reductions are seen primarily in the parietal lobes and in the lateral occipital cortices, while at age 20, relatively larger reductions are seen laterally in the frontal lobes and the inferior parietal and temporal cortices, as well as in anterior medial frontal areas.

The cerebral cortex and subcortical structures in development

Longitudinal volume reductions were found across almost the entire cortical surface. Annual change rates varied, but exceeded 1.0% in several regions and were substantially higher in the parietal lobes and in the dorsolateral prefrontal and posterior lateral temporal cortices. The results are largely consistent with previous studies on both cortical volume and thickness (Giedd et al., 1999; Raznahan et al., 2011b; Shaw et al., 2008; Sowell et al., 2004; Sullivan et al., 2011; Tamnes et al., 2010). For instance, in a recent longitudinal twin study (van Soelen et al., 2012), the average cortical thinning across the surface from age 9 to 12 years was 1.5%, and effects were observed across the parietal and lateral occipital cortices, as well as in several frontal areas. The pattern of postnatal cortical expansion has intriguingly been shown to be similar to the pattern of human evolutionary expansion (Hill et al., 2010), indicating that certain phylogenetic mechanisms may be recapitulated during ontogeny.

There has been less focus on subcortical structures, and results for specific structures are still inconclusive. For example, while significant frontal and parietal cortical reductions were seen, subcortical structures did not show consistent changes in a recent study (Sullivan et al., 2011). Other longitudinal studies have focused exclusively on the caudate (Lenroot et al., 2007), the hippocampus (Gogtay et al., 2006; Mattai et al., 2011) or the cerebellum (Tiemeier et al., 2010). Here, we found volume decreases for most of the subcortical structures and the cerebellar cortex, while the brainstem and the lateral ventricles increased. The cortical reductions were however markedly greater than the subcortical changes, in coherence with the results from Sullivan et al. (2011). Thus, it seems that even though significant maturation is evident for the subcortical structures in this age-range, the cortical changes are more prominent.

Of the subcortical structures, the caudate, accumbens and putamen changed the most, while the hippocampus and amygdala showed only small decreases. The results are generally in line with our previous cross-sectional study (Østby et al., 2009), with two exceptions. First, in the current study the thalamus decreased with age, while no age-related differences were found in the cross-sectional study. Second, in the cross-sectional sample, small volume increases were indicated for the hippocampus and amygdala. Despite diverging effects across studies (Giedd et al., 1996b; Guo et al., 2007; Mattai et al., 2011; Sowell et al., 2002), it seems that the amygdala and hippocampus develop at a different pace than other structures. Future studies should delineate developmental effects in specific hippocampal subfields (Van Leemput et al., 2009), as heterogeneous trajectories for the posterior and anterior subregions have been found (Gogtay et al., 2006).

An imperative question is to what degree changes in different cortical and subcortical regions are coordinated. In a previous cross-sectional

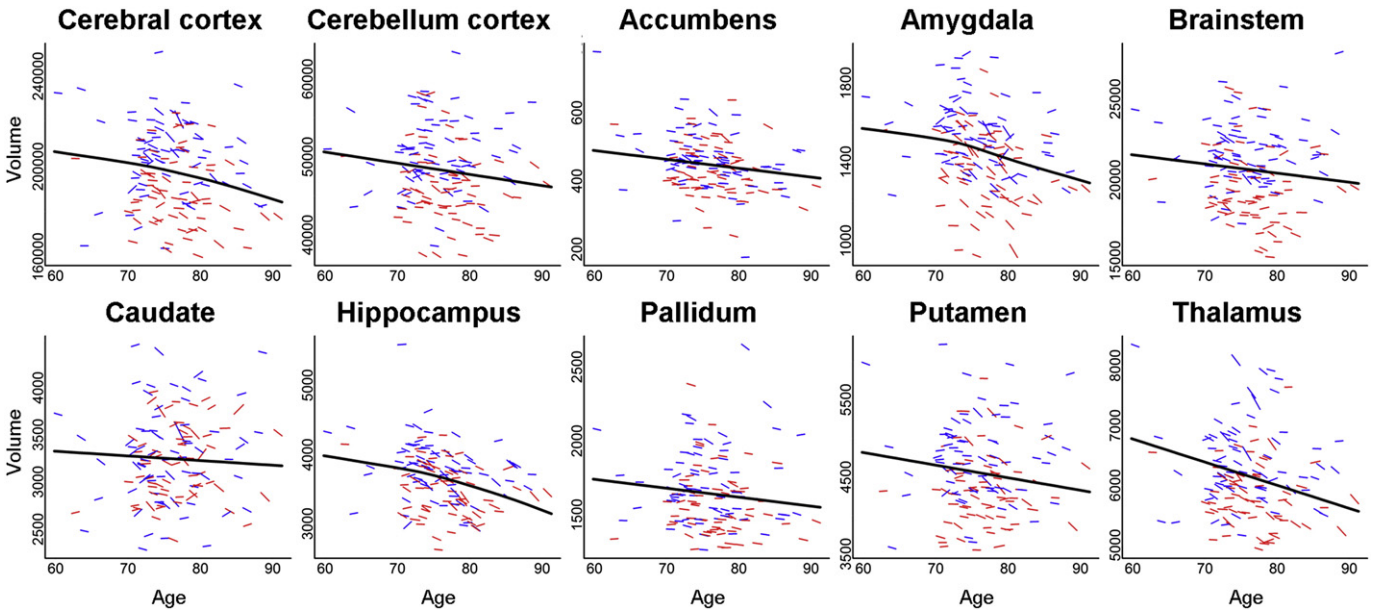

Fig. 6. Spaghetti plots for selected brain regions in aging. Plots of volumes (mm^3) by age (years) for selected brain regions in the sample of elderly (n = 142, 60–91 years). Volumes from the left and right hemispheres were averaged. Blue lines denote males and red lines denote females. For each region, an assumption-free general additive model as a function of age was fitted to accurately describe changes across the age-range.

study (Tamnes et al., 2010), we found that varied structural metrics are complementary and only somewhat correlated. Cortical thickness, WM volume and diffusion tensor imaging indices all showed unique associations with age, but only moderate regional associations with each other (Tamnes et al., 2010). In an elegant recent study, Raznahan et al. (2011a) found that regional rates of cortical development are highly organized with respect to one another and differ systematically in magnitude between higher- and lower-order cortices. Although the factors that contribute to these patterns remain unclear, it is suggested that fronto-temporal cortices show elevated degrees of maturational coupling because they subserve integrative processes that require greater functional coordination across regions (Raznahan et al., 2011a). Regional cortical development should also be deconstructed, as changes in cortical volume arise through a complex interplay of several distinct facets of anatomy (Raznahan et al., 2011b), including thickness, surface area and degree of gyrification (Hogstrom et al., in press; Mills et al., in press; White et al., 2010). This is of particular interest given that the genetic influences on thickness and arealization are known to be largely non-overlapping (Eyler et al., 2011; Panizzon et al., 2009). Future studies should also investigate hemispheric differences in longitudinal cortical change in childhood and adolescence in greater detail, as the current results showed somewhat larger volume reductions in selected temporal and medial parietal regions in the left hemisphere and larger reductions in selected frontal and lateral parietal regions in the right hemisphere.

Patterns of change across development and aging

Importantly, the results showed steeper developmental trajectories in posterior cortical regions in childhood and steeper trajectories in frontal regions in adolescence, supporting the proposition that cortical maturation in general progresses in a posterior-to-anterior order (Jernigan et al., 2011). This has previously been indicated by studies showing that reductions appear first in primary sensory-motor cortices, then in secondary areas and finally in polymodal association areas (Gogtay et al., 2004; Shaw et al., 2008). Parallels between this pattern and milestones in cognitive development have been suggested (Casey et al., 2005). Of great importance, however, is how trajectories of change across development relate to the atrophic changes in aging (Toga et al., 2006). Specifically, the relevance of developmental patterns for healthy aging and dementia has been conceptualized in terms of retrogenesis (Reisberg et al., 1999). Deterioration or degenerative mechanisms are thought to proceed inversely to ontogenic acquisition patterns, i.e. systems that are last to mature in development will be more vulnerable to aging and disease in the other end of the lifespan. The present report is the first to combine longitudinal data from samples of children and adolescents (n = 85, 8–22 years) and elderly (n = 142, 60–91 years) and directly contrast cortical and subcortical changes in maturation and senescence. The results revealed substantially greater cortical reductions in development than in aging, with the annual volume decreases two–three times larger in children and adolescents in most regions. In contrast, larger ventricular volume increases were seen in aging. For the subcortical structures, the results were more mixed, with larger decline in development in the caudate and greater atrophy rates in aging in the amygdala and hippocampus. An important question regards the extent to which atrophy in the elderly sample reflects normal aging or instances of subclinical conditions such as preclinical dementia. As neurodegenerative conditions may manifest in the brain years before clinical symptoms are detectable, follow-up data over several years are needed to rule out with certainty that disease processes caused some of the observed atrophy. Still, previous studies have demonstrated that even participants with the highest degree of stability on neuropsychological tests show significant longitudinal brain changes (Fjell et al., 2010b), so we believe that the present results do not reflect subclinical age-related neurodegenerative conditions.

A comparison of relative rates of cortical change in development and in elderly revealed a mixture of overlapping and unique characterizing changes in maturation and senescence. On the lateral surface, the most pronounced cortical reductions in development and in aging were anatomically similar. However, on the medial surface, we found spatially distinct patterns of change in the medial frontal and temporal lobes. Furthermore, comparisons of childhood development vs. aging and adolescent development vs. aging revealed striking transitions from highly different patterns of cortical reductions in early development and aging, to much more similar patterns of change in late development and aging. This was especially prominent in the medial orbitofrontal cortex, and indicates a pattern where late developed

Table 2
Annual longitudinal change in development (n = 85, 8–22 years) and aging (n = 142, 60–91 years) compared.

	Mean annual change (%)		Group difference		
	Development	Aging	t	p	Ratio
Brain structures					
Cerebral cortex	−1.15	−0.40	**9.09**	$<10^{-17}$	2.9
Cerebellum cortex	−0.58	−0.35	3.20	.002	1.7
Accumbens	−0.62	−0.57	0.46	.647	1.1
Amygdala	−0.16	−0.82	**−4.79**	$<10^{-6}$	0.2
Brainstem	0.52	−0.31	**−9.05**	$<10^{-17}$	1.7
Caudate	−0.82	−0.24	**4.69**	$<10^{-6}$	3.4
Hippocampus	−0.16	−0.84	**−6.14**	$<10^{-9}$	0.2
Pallidum	−0.20	−0.40	−3.14	.002	0.5
Putamen	−0.60	−0.43	2.37	.019	1.4
Thalamus	−0.44	−0.69	−2.97	.003	0.6
Ventricles					
Lateral ventricle	1.92	4.40	**4.05**	$<10^{-5}$	0.4
Inferior lateral ventricle	0.47	5.47	**7.63**	$<10^{-12}$	0.1
3rd ventricle	1.03	3.07	**3.35**	<.001	0.3
4th ventricle	0.02	0.71	1.78	.077	<0.1
Cortical regions					
Cingulate, rostral anterior	−0.73	−0.34	**4.34**	$<10^{-5}$	2.1
Cingulate, caudal anterior	−0.80	−0.27	**5.99**	$<10^{-9}$	3.0
Cingulate, posterior	−1.11	−0.25	**9.54**	$<10^{-18}$	4.4
Cingulate, retrosplenial	−1.00	−0.20	**10.05**	$<10^{-20}$	5.0
Frontal, superior	−0.76	−0.31	**4.46**	$<10^{-5}$	2.5
Frontal, caudal middle	−0.94	−0.40	**5.11**	$<10^{-7}$	2.4
Frontal, rostral middle	−1.26	−0.32	**7.83**	$<10^{-13}$	3.9
Frontal, pars opercularis	−1.11	−0.38	**7.91**	$<10^{-13}$	2.9
Frontal, pars triangularis	−1.18	−0.37	**7.44**	$<10^{-12}$	3.2
Frontal, pars orbitalis	−0.91	−0.38	**4.59**	$<10^{-6}$	2.4
Frontal, lateral orbital	−0.84	−0.42	**4.54**	$<10^{-6}$	2.0
Frontal, medial orbital	−0.85	−0.39	**4.77**	$<10^{-6}$	2.2
Frontal, pole	−0.47	−0.59	−0.62	.539	0.8
Frontal, precentral	−0.49	−0.10	**4.12**	$<10^{-5}$	4.9
Parietal, postcentral	−0.93	0.09	**11.83**	$<10^{-25}$	10.3
Parietal, paracentral	−0.78	−0.17	**6.54**	$<10^{-10}$	4.6
Parietal, superior	−1.24	−0.18	**10.76**	$<10^{-22}$	6.9
Parietal, inferior	−1.57	−0.40	**11.24**	$<10^{-23}$	3.9
Parietal, supramarginal	−1.47	−0.38	**9.93**	$<10^{-19}$	3.9
Parietal, precuneus	−1.36	−0.30	**12.16**	$<10^{-26}$	4.5
Temporal, parahippocampal	−0.68	−0.36	**3.61**	$<10^{-4}$	1.9
Temporal, entorhinal	−0.04	−0.55	**−4.15**	$<10^{-5}$	0.1
Temporal, pole	0.11	−0.56	**−4.52**	$<10^{-6}$	0.2
Temporal, superior	−0.95	−0.43	**5.89**	$<10^{-8}$	2.2
Temporal, middle	−1.30	−0.47	**7.38**	$<10^{-12}$	2.8
Temporal, inferior	−1.11	−0.47	**6.47**	$<10^{-10}$	2.4
Temporal, transverse	−0.79	−0.31	**5.22**	$<10^{-7}$	2.6
Temporal, banks sup temp sulcus	−1.43	−0.55	**8.89**	$<10^{-16}$	2.6
Temporal, fusiform	−0.94	−0.38	**7.30**	$<10^{-12}$	2.5
Occipital, lateral	−1.10	−0.19	**10.41**	$<10^{-21}$	5.8
Occipital, cuneus	−0.80	−0.04	**10.83**	$<10^{-22}$	20.0
Occipital, pericalcarine	−0.56	0.11	**9.53**	$<10^{-18}$	5.1
Occipital, lingual	−0.80	−0.02	**12.05**	$<10^{-26}$	40.0

The significance of the difference in annual percentage volume change in each region in development and aging was tested with independent samples t-tests. Bold: p<.05 (Bonferroni-corrected, factor of 47). Ratios were calculated by dividing the mean annual change in the developmental sample on mean annual change in the aging sample.

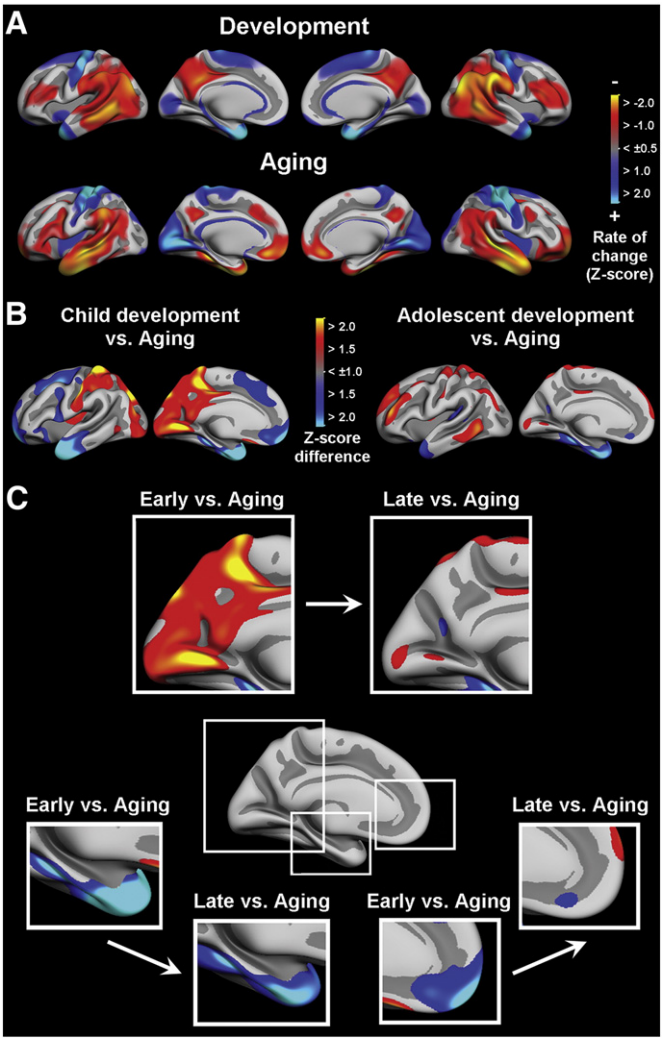

Fig. 7. Relative rates of cortical change in development and aging. A: To compare and contrast the pattern of cortical change in development and aging, the annual percentage volume change was z-transformed for each hemisphere in children and adolescents (n = 85, 8–22 years) and elderly (n = 142, 60–91 years) separately. Red–yellow areas indicate the largest relative cortical reductions within each group. The pattern of lateral cortical changes was similar in development and aging, except in the anterior part of the temporal lobes, but the characteristic pronounced medial fronto-temporal reduction in aging was not precast across development. B: Next, we calculated the differences between the smoothed estimated standardized volume changes (z-scores) in early development vs. aging (the difference between reductions at 8 years and at 75 years) and late development vs. aging (the difference between reductions at 20 years and at 75 years). Children showed larger relative parietal and occipital reductions than elderly participants, while the elderly showed larger frontal and temporal reductions. The patterns of relative changes in adolescent development and aging were much more similar, with the exception of the pronounced medial temporal reductions in aging. C: Highlights of some of the striking transitions from the relatively large differences between early development and aging to the much more similar changes taking place in late development and aging. Note the deviant pattern in the medial temporal lobe. Only the left hemisphere is shown in panels B and C, but results for the right hemisphere were similar.

cortical areas are more vulnerable to atrophy in healthy aging. A similar link has been suggested in relation to AD, and it has been speculated that the last systems to mature are characterized by high degrees of plasticity throughout life and that this makes them more susceptible to neurodegeneration (Mesulam, 2000; Thompson et al., 2003; Toga et al., 2006). The notable exception to the general pattern of late maturing areas being most affected by atrophy in aging was the medial temporal cortex, including the hippocampus and amygdala. These areas were characterized by very modest changes across development, as also reported in previous research (Shaw et al., 2008; van Soelen et al., 2012), but high degrees of atrophy in aging. Although medial temporal lobe structures show a high degree of plasticity well into old age (Buell and Coleman, 1981; Flood et al., 1985; Ming and Song, 2011), the suggested pattern of coordinated change in development and aging is not reflected here.

The spatially distinct patterns of change support that cortical reductions in development and atrophy in aging reflect partly different underlying processes (Sowell et al., 2003; Westlye et al., 2010a). The cellular and molecular mechanisms causing structural changes in childhood and adolescence are not fully understood, but there is evidence for at least two concurrent processes: dynamic synaptic reorganization, including reductions of synaptic density in the cortex

(Huttenlocher and Dabholkar, 1997; Petanjek et al., 2011) and continued myelination of the axons (Benes, 1989; Benes et al., 1994; Yakovlev and Lecours, 1967). During the course of development the brain likely sacrifices plasticity for the sake of efficiency and stability. Pruning of underutilized connections may result in a loss of plasticity, while strengthening of the remaining synapses and increased caliber and myelination of highly used axons result in increased efficiency and consistency of signal transmission (Blakemore, 2012; Tau and Peterson, 2010), which is even observed at the behavioral level (Tamnes et al., 2012). Topographical differences have been found in the time course for both synapse formation/elimination and myelination (Webb et al., 2001), but the links with regional macrostructural changes are not well understood. In aging, reductions in the number of synaptic spines and synapses, as well as shrinkage of cell bodies, are thought to be relevant factors (Esiri, 2007; Freeman et al., 2008; Jacobs et al., 1997; Pereira et al., 2007). An important task for further research is to disentangle to what degree common mechanisms may be responsible for brain maturation in childhood and degenerative changes in aging (Nikolaev et al., 2009; Wines-Samuelson and Shen, 2005), and to what degree distinct processes are causing the observed macrostructural changes. Longitudinal studies should utilize multimodal and multidimensional data to explore the relationships between morphometric measures, water diffusivity and signal intensity and tissue contrast in development and aging (Brown and Jernigan, 2012; Groves et al., 2012; Kumar et al., 2012; Salat et al., 2009; Westlye et al., 2009, 2010a), as this could indirectly inform us on the underlying specific biological processes that give rise to the imaging effects. Intriguingly, a recent cross-sectional study (Brown et al., 2012) found that different imaging modalities contribute most strongly to predicting age over the course of development, indicating a dynamic cascade of changes with different features dominating at different points.

Conclusions

The present study demonstrates differing rates of change across brain structures and regions in development, as well as accelerating cortical change in frontal areas and decelerating change in posterior areas, supporting that maturation in general proceeds in a "posterior-to-anterior" direction. Comparisons of children and elderly revealed a mixture of overlapping and spatially distinct patterns of change in maturation and senescence, and indicated that late developed cortical areas are more vulnerable to late-life atrophy, although an important exception from this principle was seen in the medial temporal lobe.

Supplementary data to this article can be found online at http://dx.doi.org/10.1016/j.neuroimage.2012.11.039.

Disclosure statement

Anders M. Dale is a founder and holds equity in CorTechs Labs, Inc., and also serves on the Scientific Advisory Board. The terms of this arrangement have been reviewed and approved by the University of California, San Diego, in accordance with its conflict of interest policies.

Acknowledgments

Funding: The Norwegian Research Council (177404 and 186092 to KBW; 189507 and 199537 to AMF; 204966 to LTW), the European Research Council (283634 to AMF), the University of Oslo (to CKT, KBW and AMF), and the U.S.–Norway Fulbright Foundation (to CKT). ADNI (PI: Michael Weiner; NIH grant U01 AG024904) is funded by the National Institute on Aging, the National Institute of Biomedical Imaging and Bioengineering, and through contributions from the following: Abbott; Alzheimer's Association; Alzheimer's Drug Discovery Foundation; Amorfix Life Sciences Ltd.; AstraZeneca; Bayer HealthCare; BioClinica, Inc.; Biogen Idec Inc.; Bristol-Myers Squibb Company; Eisai Inc.; Elan Pharmaceuticals Inc.; Eli Lilly and Company; F. Hoffmann-La Roche Ltd and Genentech, Inc.; GE Healthcare; Innogenetics, N.V.; Janssen Alzheimer Immunotherapy Research & Development, LLC.; Johnson & Johnson Pharmaceutical Research & Development LLC.; Medpace, Inc.; Merck & Co., Inc.; Meso Scale Diagnostics, LLC.; Novartis Pharmaceuticals Corporation; Pfizer Inc.; Servier; Synarc Inc.; and Takeda Pharmaceutical Company. The Canadian Institutes of Health Research is providing funds to support clinical sites in Canada. Private sector contributions are facilitated by the Foundation for the National Institutes of Health. The grantee organization is the Northern California Institute for Research and Education, and the study is coordinated by the Alzheimer's Disease Cooperative Study at the UCSD. ADNI data are disseminated by the Laboratory for Neuro Imaging at the UCLA. ADNI is also supported by NIH grants P30 AG010129 and K01 AG030514.

References

Benes, F.M., 1989. Myelination of cortical–hippocampal relays during late adolescence. Schizophr. Bull. 15, 585–593.
Benes, F.M., Turtle, M., Khan, Y., Farol, P., 1994. Myelination of a key relay zone in the hippocampal formation occurs in the human brain during childhood, adolescence, and adulthood. Arch. Gen. Psychiatry 51, 477–484.
Blakemore, S.J., 2012. Imaging brain development: the adolescent brain. NeuroImage 61, 397–406.
Brain Development Cooperative Group, 2012. Total and regional brain volumes in a population-based normative sample from 4 to 18 years: the NIH MRI study of normal brain development. Cereb. Cortex 22, 1–12.
Brown, T.T., Jernigan, T.L., 2012. Brain development during the preschool years. Neuropsychol. Rev. 22, 313–333.
Brown, T.T., et al., 2012. Neuroanatomical assessment of biological maturity. Curr. Biol. 22, 1693–1698.
Buell, S.J., Coleman, P.D., 1981. Quantitative evidence for selective dendritic growth in normal human aging but not in senile dementia. Brain Res. 214, 23–41.
Casey, B.J., Tottenham, N., Liston, C., Durston, S., 2005. Imaging the developing brain: what have we learned about cognitive development? Trends Cogn. Sci. 9, 104–110.
Dale, A.M., Fischl, B., Sereno, M.I., 1999. Cortical surface-based analysis. I. Segmentation and surface reconstruction. NeuroImage 9, 179–194.
Deary, I.J., Bastin, M.E., Pattie, A., Clayden, J.D., Whalley, L.J., Starr, J.M., Wardlaw, J.M., 2006. White matter integrity and cognition in childhood and old age. Neurology 66, 505–512.
Desikan, R.S., Segonne, F., Fischl, B., Quinn, B.T., Dickerson, B.C., Blacker, D., Buckner, R.L., Dale, A.M., Maguire, R.P., Hyman, B.T., Albert, M.S., Killiany, R.J., 2006. An automated labeling system for subdividing the human cerebral cortex on MRI scans into gyral based regions of interest. NeuroImage 31, 968–980.
Esiri, M.M., 2007. Ageing and the brain. J. Pathol. 211, 181–187.
Eyler, L.T., et al., 2011. Genetic and environmental contributions to regional cortical surface area in humans: a magnetic resonance imaging twin study. Cereb. Cortex 21, 2313–2321.
Fennema-Notestine, C., Hagler Jr., D.J., McEvoy, L.K., Fleisher, A.S., Wu, E.H., Karow, D.S., Dale, A.M., 2009. Structural MRI biomarkers for preclinical and mild Alzheimer's disease. Hum. Brain Mapp. 30, 3238–3253.
Fischl, B., Dale, A.M., 2000. Measuring the thickness of the human cerebral cortex from magnetic resonance images. Proc. Natl. Acad. Sci. U. S. A. 97, 11050–11055.
Fischl, B., Sereno, M.I., Dale, A.M., 1999. Cortical surface-based analysis. II: inflation, flattening, and a surface-based coordinate system. NeuroImage 9, 195–207.
Fischl, B., Salat, D.H., Busa, E., Albert, M., Dieterich, M., Haselgrove, C., van der Kouwe, A., Killiany, R., Kennedy, D., Klaveness, S., Montillo, A., Makris, N., Rosen, B., Dale, A.M., 2002. Whole brain segmentation: automated labeling of neuroanatomical structures in the human brain. Neuron 33, 341–355.
Fischl, B., van der Kouwe, A., Destrieux, C., Halgren, E., Segonne, F., Salat, D.H., Busa, E., Seidman, L.J., Goldstein, J., Kennedy, D., Caviness, V., Makris, N., Rosen, B., Dale, A.M., 2004. Automatically parcellating the human cerebral cortex. Cereb. Cortex 14, 11–22.
Fjell, A.M., Walhovd, K.B., 2010. Structural brain changes in aging: courses, causes and cognitive consequences. Rev. Neurosci. 21, 187–221.
Fjell, A.M., Walhovd, K.B., Fennema-Notestine, C., McEvoy, L.K., Hagler, D.J., Holland, D., Brewer, J.B., Dale, A.M., 2009a. One-year brain atrophy evident in healthy aging. J. Neurosci. 29, 15223–15231.
Fjell, A.M., Westlye, L.T., Amlien, I., Espeseth, T., Reinvang, I., Raz, N., Agartz, I., Salat, D.H., Greve, D.N., Fischl, B., Dale, A.M., Walhovd, K.B., 2009b. High consistency of regional cortical thinning in aging across multiple samples. Cereb. Cortex 19, 2001–2012.
Fjell, A.M., Walhovd, K.B., Westlye, L.T., Østby, Y., Tamnes, C.K., Jernigan, T.L., Gamst, A., Dale, A.M., 2010a. When does brain aging accelerate? Dangers of quadratic fits in cross-sectional studies. NeuroImage 50, 1376–1383.
Fjell, A.M., Westlye, L.T., Espeseth, T., Reinvang, I., Dale, A.M., Holland, D., Walhovd, K.B., 2010b. Cortical gray matter atrophy in healthy aging cannot be explained by undetected incipient cognitive disorders: a comment on Burgmans et al. (2009). Neuropsychology 24, 258–263 (discussion 264–266).
Flood, D.G., Buell, S.J., Defiore, C.H., Horwitz, G.J., Coleman, P.D., 1985. Age-related dendritic growth in dentate gyrus of human brain is followed by regression in the 'oldest old'. Brain Res. 345, 366–368.

Folstein, M.F., Folstein, S.E., McHugh, P.R., 1975. “Mini-mental state”. A practical method for grading the cognitive state of patients for the clinician. J. Psychiatr. Res. 12, 189–198.
Freeman, S.H., Kandel, R., Cruz, L., Rozkalne, A., Newell, K., Frosch, M.P., Hedley-Whyte, E.T., Locascio, J.J., Lipsitz, L.A., Hyman, B.T., 2008. Preservation of neuronal number despite age-related cortical brain atrophy in elderly subjects without Alzheimer disease. J. Neuropathol. Exp. Neurol. 67, 1205–1212.
Genovese, C.R., Lazar, N.A., Nichols, T., 2002. Thresholding of statistical maps in functional neuroimaging using the false discovery rate. NeuroImage 15, 870–878.
Giedd, J.N., Rapoport, J.L., 2010. Structural MRI of pediatric brain development: what have we learned and where are we going? Neuron 67, 728–734.
Giedd, J.N., Snell, J.W., Lange, N., Rajapakse, J.C., Casey, B.J., Kozuch, P.L., Vaituzis, A.C., Vauss, Y.C., Hamburger, S.D., Kaysen, D., Rapoport, J.L., 1996a. Quantitative magnetic resonance imaging of human brain development: ages 4–18. Cereb. Cortex 6, 551–560.
Giedd, J.N., Vaituzis, A.C., Hamburger, S.D., Lange, N., Rajapakse, J.C., Kaysen, D., Vauss, Y.C., Rapoport, J.L., 1996b. Quantitative MRI of the temporal lobe, amygdala, and hippocampus in normal human development: ages 4–18 years. J. Comp. Neurol. 366, 223–230.
Giedd, J.N., Blumenthal, J., Jeffries, N.O., Castellanos, F.X., Liu, H., Zijdenbos, A., Paus, T., Evans, A.C., Rapoport, J.L., 1999. Brain development during childhood and adolescence: a longitudinal MRI study. Nat. Neurosci. 2, 861–863.
Gilmore, J.H., Shi, F., Woolson, S.L., Knickmeyer, R.C., Short, S.J., Lin, W., Zhu, H., Hamer, R.M., Styner, M., Shen, D., 2012. Longitudinal development of cortical and subcortical gray matter from birth to 2 years. Cereb. Cortex 22, 2478–2485.
Gogtay, N., Giedd, J.N., Lusk, L., Hayashi, K.M., Greenstein, D., Vaituzis, A.C., Nugent, T.F., Herman, D.H., Clasen, L.S., Toga, A.W., Rapoport, J.L., Thompson, P.M., 2004. Dynamic mapping of human cortical development during childhood through early adulthood. Proc. Natl. Acad. Sci. U. S. A. 101, 8174–8179.
Gogtay, N., Nugent, T.F., Herman, D.H., Ordonez, A., Greenstein, D., Hayashi, K.M., Clasen, L., Toga, A.W., Giedd, J.N., Rapoport, J.L., Thompson, P.M., 2006. Dynamic mapping of normal human hippocampal development. Hippocampus 16, 664–672.
Gogtay, N., Vyas, N.S., Testa, R., Wood, S.J., Pantelis, C., 2011. Age of onset of schizophrenia: perspectives from structural neuroimaging studies. Schizophr. Bull. 37, 504–513.
Groves, A.R., Smith, S.M., Fjell, A.M., Tamnes, C.K., Walhovd, K.B., Douaud, G., Woolrich, M.W., Westlye, L.T., 2012. Benefits of multi-modal fusion analysis on a large-scale dataset: life-span patterns of inter-subject variability in cortical morphometry and white matter microstructure. NeuroImage 63, 365–380.
Guo, X., Chen, C., Chen, K., Jin, Z., Peng, D., Yao, L., 2007. Brain development in Chinese children and adolescents: a structural MRI study. Neuroreport 18, 875–880.
Han, X., Jovicich, J., Salat, D., van der Kouwe, A., Quinn, B., Czanner, S., Busa, E., Pacheco, J., Albert, M., Killiany, R., Maguire, P., Rosas, D., Makris, N., Dale, A., Dickerson, B., Fischl, B., 2006. Reliability of MRI-derived measurements of human cerebral cortical thickness: the effects of field strength, scanner upgrade and manufacturer. NeuroImage 32, 180–194.
Hill, J., Inder, T., Neil, J., Dierker, D., Harwell, J., Van Essen, D., 2010. Similar patterns of cortical expansion during human development and evolution. Proc. Natl. Acad. Sci. U. S. A. 107, 13135–13140.
Hogstrom, L.J., Westlye, L.T., Walhovd, K.B., Fjell, A.M., in press. The structure of the cerebral cortex across adult life: age-related patterns of surface area, thickness, and gyrification. Cereb. Cortex.
Holland, D., Dale, A.M., 2011. Nonlinear registration of longitudinal images and measurement of change in regions of interest. Med. Image Anal. 15, 489–497.
Holland, D., Brewer, J.B., Hagler, D.J., Fennema-Notestine, C., Dale, A.M., 2009. Subregional neuroanatomical change as a biomarker for Alzheimer's disease. Proc. Natl. Acad. Sci. U. S. A. 106, 20954–20959.
Holland, D., McEvoy, L.K., Dale, A.M., 2012. Unbiased comparison of sample size estimates from longitudinal structural measures in ADNI. Hum. Brain Mapp. 33, 2586–2602.
Huttenlocher, P.R., Dabholkar, A.S., 1997. Regional differences in synaptogenesis in human cerebral cortex. J. Comp. Neurol. 387, 167–178.
Jack Jr., C.R., et al., 2008. The Alzheimer's Disease Neuroimaging Initiative (ADNI): MRI methods. J. Magn. Reson. Imaging 27, 685–691.
Jacobs, B., Driscoll, L., Schall, M., 1997. Life-span dendritic and spine changes in areas 10 and 18 of human cortex: a quantitative Golgi study. J. Comp. Neurol. 386, 661–680.
Jernigan, T.L., Baare, W.F., Stiles, J., Madsen, K.S., 2011. Postnatal brain development: structural imaging of dynamic neurodevelopmental processes. Prog. Brain Res. 189, 77–92.
Jovicich, J., Czanner, S., Greve, D., Haley, E., van der Kouwe, A., Gollub, R., Kennedy, D., Schmitt, F., Brown, G., Macfall, J., Fischl, B., Dale, A., 2006. Reliability in multi-site structural MRI studies: effects of gradient non-linearity correction on phantom and human data. NeuroImage 30, 436–443.
Jovicich, J., Czanner, S., Han, X., Salat, D., van der Kouwe, A., Quinn, B., Pacheco, J., Albert, M., Killiany, R., Blacker, D., Maguire, P., Rosas, D., Makris, N., Gollub, R., Dale, A., Dickerson, B.C., Fischl, B., 2009. MRI-derived measurements of human subcortical, ventricular and intracranial brain volumes: reliability effects of scan sessions, acquisition sequences, data analyses, scanner upgrade, scanner vendors and field strengths. NeuroImage 46, 177–192.
Knickmeyer, R.C., Gouttard, S., Kang, C., Evans, D., Wilber, K., Smith, J.K., Hamer, R.M., Lin, W., Gerig, G., Gilmore, J.H., 2008. A structural MRI study of human brain development from birth to 2 years. J. Neurosci. 28, 12176–12182.
Kochunov, P., Williamson, D.E., Lancaster, J., Fox, P., Cornell, J., Blangero, J., Glahn, D.C., 2012. Fractional anisotropy of water diffusion in cerebral white matter across the lifespan. Neurobiol. Aging 33, 9–20.
Kumar, R., Delshad, S., Woo, M.A., Macey, P.M., Harper, R.M., 2012. Age-related regional brain T2-relaxation changes in healthy adults. J. Magn. Reson. Imaging 35 (2), 300–308.
Lemaitre, H., Goldman, A.L., Sambataro, F., Verchinski, B.A., Meyer-Lindenberg, A., Weinberger, D.R., Mattay, V.S., 2012. Normal age-related brain morphometric changes: nonuniformity across cortical thickness, surface area and gray matter volume? Neurobiol. Aging 33 (617), e611–e619.
Lenroot, R.K., Gogtay, N., Greenstein, D.K., Wells, E.M., Wallace, G.L., Clasen, L.S., Blumenthal, J.D., Lerch, J., Zijdenbos, A.P., Evans, A.C., Thompson, P.M., Giedd, J.N., 2007. Sexual dimorphism of brain developmental trajectories during childhood and adolescence. NeuroImage 36, 1065–1073.
Mattai, A., Hosanagar, A., Weisinger, B., Greenstein, D., Stidd, R., Clasen, L., Lalonde, F., Rapoport, J., Gogtay, N., 2011. Hippocampal volume development in healthy siblings of childhood-onset schizophrenia patients. Am. J. Psychiatry 168, 427–435.
McEvoy, L.K., Holland, D., Hagler Jr., D.J., Fennema-Notestine, C., Brewer, J.B., Dale, A.M., 2011. Mild cognitive impairment: baseline and longitudinal structural MR imaging measures improve predictive prognosis. Radiology 259, 834–843.
Mesulam, M.M., 2000. A plasticity-based theory of the pathogenesis of Alzheimer's disease. Ann. N. Y. Acad. Sci. 924, 42–52.
Mills, K.L., Lalonde, F., Clasen, L., Giedd, J.N., Blakemore, S.J., in press. Developmental changes in the structure of the social brain in late childhood and adolescence. Soc. Cogn. Affect. Neurosci.
Ming, G.L., Song, H., 2011. Adult neurogenesis in the mammalian brain: significant answers and significant questions. Neuron 70, 687–702.
Morris, J.C., 1993. The Clinical Dementia Rating (CDR): current version and scoring rules. Neurology 43, 2412–2414.
Muftuler, L.T., Davis, E.P., Buss, C., Head, K., Hasso, A.N., Sandman, C.A., 2011. Cortical and subcortical changes in typically developing preadolescent children. Brain Res. 1399, 15–24.
Murphy, E.A., Holland, D., Donohue, M., McEvoy, L.K., Hagler Jr., D.J., Dale, A.M., Brewer, J.B., 2010. Six-month atrophy in MTL structures is associated with subsequent memory decline in elderly controls. NeuroImage 53, 1310–1317.
Nikolaev, A., McLaughlin, T., O'Leary, D.D., Tessier-Lavigne, M., 2009. APP binds DR6 to trigger axon pruning and neuron death via distinct caspases. Nature 457, 981–989.
Østby, Y., Tamnes, C.K., Fjell, A.M., Westlye, L.T., Due-Tønnessen, P., Walhovd, K.B., 2009. Heterogeneity in subcortical brain development: a structural magnetic resonance imaging study of brain maturation from 8 to 30 years. J. Neurosci. 29, 11772–11782.
Panizzon, M.S., Fennema-Notestine, C., Eyler, L.T., Jernigan, T.L., Prom-Wormley, E., Neale, M., Jacobson, K., Lyons, M.J., Grant, M.D., Franz, C.E., Xian, H., Tsuang, M., Fischl, B., Seidman, L., Dale, A., Kremen, W.S., 2009. Distinct genetic influences on cortical surface area and cortical thickness. Cereb. Cortex 19, 2728–2735.
Paus, T., Keshavan, M., Giedd, J.N., 2008. Why do many psychiatric disorders emerge during adolescence? Nat. Rev. Neurosci. 9, 947–957.
Pereira, A.C., Wu, W., Small, S.A., 2007. Imaging-guided microarray: isolating molecular profiles that dissociate Alzheimer's disease from normal aging. Ann. N. Y. Acad. Sci. 1097, 225–238.
Petanjek, Z., Judas, M., Simic, G., Rasin, M.R., Uylings, H.B., Rakic, P., Kostovic, I., 2011. Extraordinary neoteny of synaptic spines in the human prefrontal cortex. Proc. Natl. Acad. Sci. U. S. A. 108, 13281–13286.
Raznahan, A., Lerch, J.P., Lee, N., Greenstein, D., Wallace, G.L., Stockman, M., Clasen, L., Shaw, P.W., Giedd, J.N., 2011a. Patterns of coordinated anatomical change in human cortical development: a longitudinal neuroimaging study of maturational coupling. Neuron 72, 873–884.
Raznahan, A., Shaw, P., Lalonde, F., Stockman, M., Wallace, G.L., Greenstein, D., Clasen, L., Gogtay, N., Giedd, J.N., 2011b. How does your cortex grow? J. Neurosci. 31, 7174–7177.
Reisberg, B., Franssen, E.H., Hasan, S.M., Monteiro, I., Boksay, I., Souren, L.E., Kenowsky, S., Auer, S.R., Elahi, S., Kluger, A., 1999. Retrogenesis: clinical, physiologic, and pathologic mechanisms in brain aging, Alzheimer's and other dementing processes. Eur. Arch. Psychiatry Clin. Neurosci. 249 (Suppl. 3), 28–36.
Salat, D.H., Lee, S.Y., van der Kouwe, A.J., Greve, D.N., Fischl, B., Rosas, H.D., 2009. Age-associated alterations in cortical gray and white matter signal intensity and gray to white matter contrast. NeuroImage 48, 21–28.
Shaw, P., Lerch, J.P., Pruessner, J.C., Taylor, K.N., Rose, A.B., Greenstein, D., Clasen, L., Evans, A., Rapoport, J.L., Giedd, J.N., 2007. Cortical morphology in children and adolescents with different apolipoprotein E gene polymorphisms: an observational study. Lancet Neurol. 6, 494–500.
Shaw, P., Kabani, N.J., Lerch, J.P., Eckstrand, K., Lenroot, R., Gogtay, N., Greenstein, D., Clasen, L., Evans, A., Rapoport, J.L., Giedd, J.N., Wise, S.P., 2008. Neurodevelopmental trajectories of the human cerebral cortex. J. Neurosci. 28, 3586–3594.
Sled, J.G., Zijdenbos, A.P., Evans, A.C., 1998. A nonparametric method for automatic correction of intensity nonuniformity in MRI data. IEEE Trans. Med. Imaging 17, 87–97.
Sowell, E.R., Trauner, D.A., Gamst, A., Jernigan, T.L., 2002. Development of cortical and subcortical brain structures in childhood and adolescence: a structural MRI study. Dev. Med. Child Neurol. 44, 4–16.
Sowell, E.R., Peterson, B.S., Thompson, P.M., Welcome, S.E., Henkenius, A.L., Toga, A.W., 2003. Mapping cortical change across the human life span. Nat. Neurosci. 6, 309–315.
Sowell, E.R., Thompson, P.M., Leonard, C.M., Welcome, S.E., Kan, E., Toga, A.W., 2004. Longitudinal mapping of cortical thickness and brain growth in normal children. J. Neurosci. 24, 8223–8231.
Sullivan, E.V., Pfefferbaum, A., Rohlfing, T., Baker, F.C., Padilla, M.L., Colrain, I.M., 2011. Developmental change in regional brain structure over 7 months in early adolescence: comparison of approaches for longitudinal atlas-based parcellation. NeuroImage 57, 214–224.
Tamnes, C.K., Østby, Y., Fjell, A.M., Westlye, L.T., Due-Tønnessen, P., Walhovd, K.B., 2010. Brain maturation in adolescence and young adulthood: regional age-

related changes in cortical thickness and white matter volume and microstructure. Cereb. Cortex 20, 534–548.
Tamnes, C.K., Fjell, A.M., Westlye, L.T., Østby, Y., Walhovd, K.B., 2012. Becoming consistent: developmental reductions in intraindividual variability in reaction time are related to white matter integrity. J. Neurosci. 32, 972–982.
Tau, G.Z., Peterson, B.S., 2010. Normal development of brain circuits. Neuropsychopharmacology 35, 147–168.
Thompson, W.K., Holland, D., 2011. Bias in tensor based morphometry Stat-ROI measures may result in unrealistic power estimates. NeuroImage 57, 1–4 (discussion 5–14).
Thompson, P.M., Hayashi, K.M., de Zubicaray, G., Janke, A.L., Rose, S.E., Semple, J., Herman, D., Hong, M.S., Dittmer, S.S., Doddrell, D.M., Toga, A.W., 2003. Dynamics of gray matter loss in Alzheimer's disease. J. Neurosci. 23, 994–1005.
Tiemeier, H., Lenroot, R.K., Greenstein, D.K., Tran, L., Pierson, R., Giedd, J.N., 2010. Cerebellum development during childhood and adolescence: a longitudinal morphometric MRI study. NeuroImage 49, 63–70.
Toga, A.W., Thompson, P.M., Sowell, E.R., 2006. Mapping brain maturation. Trends Neurosci. 29, 148–159.
Van Leemput, K., Bakkour, A., Benner, T., Wiggins, G., Wald, L.L., Augustinack, J., Dickerson, B.C., Golland, P., Fischl, B., 2009. Automated segmentation of hippocampal subfields from ultra-high resolution in vivo MRI. Hippocampus 19, 549–557.
van Soelen, I.L., Brouwer, R.M., van Baal, G.C., Schnack, H.G., Peper, J.S., Collins, D.L., Evans, A.C., Kahn, R.S., Boomsma, D.I., Hulshoff Pol, H.E., 2012. Genetic influences on thinning of the cerebral cortex during development. NeuroImage 59, 3871–3880.
Walhovd, K.B., Westlye, L.T., Amlien, I., Espeseth, T., Reinvang, I., Raz, N., Agartz, I., Salat, D.H., Greve, D.N., Fischl, B., Dale, A.M., Fjell, A.M., 2011. Consistent neuroanatomical age-related volume differences across multiple samples. Neurobiol. Aging 32, 916–932.
Webb, S.J., Monk, C.S., Nelson, C.A., 2001. Mechanisms of postnatal neurobiological development: implications for human development. Dev. Neuropsychol. 19, 147–171.
Wechsler, D., 1999. Wechsler Abbreviated Scale of Intelligence (WASI). The Psychological Corporation, San Antonio (TX).
Westlye, L.T., Walhovd, K.B., Dale, A.M., Espeseth, T., Reinvang, I., Raz, N., Agartz, I., Greve, D.N., Fischl, B., Fjell, A.M., 2009. Increased sensitivity to effects of normal aging and Alzheimer's disease on cortical thickness by adjustment for local variability in gray/white contrast: a multi-sample MRI study. NeuroImage 47, 1545–1557.
Westlye, L.T., Walhovd, K.B., Dale, A.M., Bjørnerud, A., Due-Tønnessen, P., Engvig, A., Grydeland, H., Tamnes, C.K., Østby, Y., Fjell, A.M., 2010a. Differentiating maturational and aging-related changes of the cerebral cortex by use of thickness and signal intensity. NeuroImage 52, 172–185.
Westlye, L.T., Walhovd, K.B., Dale, A.M., Bjørnerud, A., Due-Tønnessen, P., Engvig, A., Grydeland, H., Tamnes, C.K., Østby, Y., Fjell, A.M., 2010b. Life-span changes of the human brain white matter: diffusion tensor imaging (DTI) and volumetry. Cereb. Cortex 20, 2055–2068.
White, T., Su, S., Schmidt, M., Kao, C.Y., Sapiro, G., 2010. The development of gyrification in childhood and adolescence. Brain Cogn. 72, 36–45.
Wines-Samuelson, M., Shen, J., 2005. Presenilins in the developing, adult, and aging cerebral cortex. Neuroscientist 11, 441–451.
Yakovlev, P.I., Lecours, A.R., 1967. The myelogenetic cycle of regional maturation of the brain. In: Minkowski, A. (Ed.), Regional Development of the Brain Early in Life. Blackwell Scientific Publications Inc., Boston (MA), pp. 3–70.